THIEME
OPEN ACCESS

Phenomenological Characterization of Low-Potency Homeopathic Preparations by Means of Pattern Formation in Evaporating Droplets

Maria Olga Kokornaczyk[1]   Sandra Würtenberger[2]   Stephan Baumgartner[1,3]

[1] Society for Cancer Research, Hiscia Institute, Arlesheim, Switzerland
[2] Scientific & Regulatory Affairs, Hevert-Arzneimittel GmbH & Co. KG, Nussbaum, Germany
[3] Institute of Integrative Medicine, University of Witten/Herdecke, Herdecke, Germany

Address for correspondence Maria Olga Kokornaczyk, PhD, Society for Cancer Research, Kirschweg 9, 4144 Arlesheim, Switzerland (e-mail: m.kokornaczyk@vfk.ch).

Abstract

Background   Evaporation-induced pattern formation in droplets has been applied to test effects of high potencies. Here we propose for the first time the droplet evaporation method (DEM) as a tool to characterize low potencies on a qualitative and quantitative basis.

Materials and Methods   The present investigation consisted of: (1) screening of 18 different substances of mineral, vegetal, and animal origin in the 1x to 6x potency range; choice of four substances with characteristic pattern-forming properties; (2) replication experiments aiming at the differentiation of four homeopathic preparations at the same potency levels (2x–6x); and (3) control experiments performed on three preparations. The DEM experimental protocol consisted of the evaporation of droplets of the analyzed potency *per se*, placed on microscope slides and in controlled conditions. The resulting patterns were photographed and subjected to computerized image analysis.

Results   The screening experiments yielded a wide variety of patterns. Homeopathic preparations of mineral origin showed the largest variety of forms, whereas potencies of vegetal origin mostly created dendritic patterns, probably due to diffusion-limited aggregation. The here-analyzed image analysis variables (gray-level distribution, entropy, and inverse difference moment) allowed a highly significant differentiation of patterns prepared from four substances (*Echinacea*, *Baptisia*, *Luffa*, and *Spongia*) at the same potency levels in the range 2x to 4x, whereas patterns obtained from potencies 5x and 6x could no longer be differentiated and resembled the pattern of pure solute (purified water). The control experiments showed reasonable experimental model stability.

Conclusions   DEM seems to be a promising tool for qualitative phenomenological characterization of homeopathic preparations in low potency. We propose the application of the current experimental model for investigating further research topics in this field, such as the comparison of potencies versus simple dilutions or the contribution of component remedies to the patterns formed by homeopathic combination medicines.

Keywords
► droplet evaporation method
► crystallization patterns
► homeopathy
► mineral extracts
► vegetal extracts
► low potencies

Introduction

In homeopathic basic research, the mainstream of studies concerns high potencies. Effects of dilutions beyond the Avogadro limit, being inconsistent with the present state of scientific knowledge, represent an interesting topic for scientific investigation. Moreover, based on Hahnemann's *Organon*,[1] the "power" of a remedy should increase with its dilution; thus, studying the effectiveness of high potencies, rather than low potencies, seems to be reasonable. From this perspective, low potencies seem to be less interesting. However, the fact that they still contain substantive material allows one to study characteristics of this very substance as well as substance-specific changes due to the successive dilution and potentization steps.

Phase-transition-induced pattern formation is a process that forms the basis of different methods applied in homeopathic basic research.[2] One such method is the droplet evaporation method (DEM), where the sample to be analyzed is applied on a substrate in the form of droplets and left for drying. The desiccated residues of such droplets, containing often surprisingly ordered patterns, comprise the main output of the method and serve as a data source for further analysis. Until now DEM was applied on three experimental models, testing high potencies: (1) evaporation of wheat seed leakage droplets prepared by soaking wheat seeds in homeopathic samples[3–6]; (2) evaporation of a droplet sequence made out of five droplets of a given homeopathic preparation, where each successive droplet is placed on the dry residue of the preceding droplet[7]; and (3) evaporation of a single droplet of a diluted (not succussed) substance.[8]

In contrast to common analytical methods aiming at isolation, identification, and quantification of defined material compounds, phase-transition-induced pattern formation is a complementary scientific approach aiming at studying and characterizing the wholeness of a given sample, which can be seen to be more than the sum of its parts. The wholeness of an element of nature is, amongst others, basically characterized by its physical form. Phenomenological science describes forms of nature by using qualitative and quantitative research methods to identify characteristic elements that are unique and specific for a given element of nature.

Here we propose a DEM experimental model consisting of the evaporation of a single droplet of a given homeopathic preparation *per se* (i.e., without any pre-treatment or addition of reagents) and apply DEM for the first time to investigate low potencies. The present study included a pilot study, where a wide choice of substances of mineral, vegetal, and animal origin, used for the preparation of homeopathic potencies, was screened by means of DEM in the potency range 1x to 6x for their pattern-forming properties. The main study aimed at testing DEM's ability to distinguish between four pre-selected substances in increasing dilution/succussion levels ranging from 2x to 6x. The image analysis consisted of calculation of the gray-level distribution (GLD) (the quantification of the gray levels across the whole image yields an estimate of the structure's size) and the textural parameters inverse difference moment (IDM) and entropy (i.e., measures of the image's homogeneity and disorder, respectively). The model was tested also for repeatability on different experimental days and for stability by means of control experiments.

Materials and Methods

Experimental Design

The experimental design (►**Fig. 1**) included a pilot study and a main study.

The pilot study consisted of screening tests, in which decimal potencies up to 6x of 18 substances (►**Table 1**) were analyzed by means of DEM regarding their pattern-forming properties. From each potency, 20 droplets were deposited on two slides, evaporated, and analyzed visually for pattern-forming properties. Based on the results of the pilot study, four substances (*Baptisia* [B], *Echinacea* [E], *Luffa* [L], and *Spongia* [S]) were chosen for the main study (selection criteria are described in the Results section).

The aim of the main study was to test DEM's capacity to differentiate between *Baptisia*, *Echinacea*, *Luffa*, and *Spongia* in five potencies, from 2x to 6x. For each potency level, one experiment (chamber run) was performed, in which the potency droplets of each of the four substances were deposited on three slides (12 slides per chamber run). Five chamber runs were performed to analyze the potencies 2x to 6x. The whole experimentation was repeated on three different experimental days. Additionally, in the potency range where DEM showed differentiation potential, control experiments (chamber runs) were performed to investigate the system stability, using potencies *Echinacea* 2x, *Baptisia* 3x, and *Luffa* 4x.

The patterns collected in the main study were subjected to computerized pattern evaluation followed by statistical analysis.

Substances for the Preparation of Investigated Potencies

All substances used in the present study were provided or manufactured according to the European Pharmacopoeia (Ph. Eur.), Homoeopathic Preparations,[9] or to the monographs in the German Homoeopathic Pharmacopoeia (GHP)[10] by Hevert-Arzneimittel GmbH & Co. KG (Nussbaum, Germany). The choice of the substances was based on both their use in the homeopathic products *Sinusitis Hevert SL* and *Calmvalera* (drops and tablets) and their diversity regarding provenance (mineral, plant, or animal origin) and expected crystallographic properties.

As shown in ►**Table 1**, the following substances were used:

- For the pilot study, 18 substances in the form of powders, mother tinctures, or 1x or 2x potencies;
- For the main study, four substances (*Baptisia, Echinacea, Luffa*, and *Spongia*) in 1x coming from the same batch as those used in the pilot study and manufactured as follows: *Baptisia* 1x and *Echinacea* 1x with method 1.1.5, *Luffa* 1x with method 1.1.8, and *Spongia* 1x with method 1.1.9.

Experimental Procedure

The experimentation was performed in the laboratories of the Society for Cancer Research (Arlesheim, Switzerland). The experimental procedure included the following steps: preparation of potencies, preparation of slides, droplet deposition

PILOT STUDY

- Screening of 18 substances (Table 1) in decimal potencies until 6x
- Preparation of patterns of the water control
- Selection of 4 substances (*Baptisia*, *Echinacea*, *Luffa*, *Spongia*) for the main experimentation

MAIN STUDY

Differentiation experiments; 5 chamber-runs

2x potencies of *Baptisia*, *Echinacea*, *Luffa*, *Spongia*; 3 slides per each potency

3x potencies of *Baptisia*, *Echinacea*, *Luffa*, *Spongia*; 3 slides per each potency

4x potencies of *Baptisia*, *Echinacea*, *Luffa*, *Spongia*; 3 slides per each potency

5x potencies of *Baptisia*, *Echinacea*, *Luffa*, *Spongia*; 3 slides per each potency

6x potencies of *Baptisia*, *Echinacea*, *Luffa*, *Spongia*; 3 slides per each potency

Control experiments; 3 chamber-runs

Echinacea 2x; 12 slides

Baptisia 3x; 12 slides

Luffa 4x; 12 slides

DATA EXTRACTION AND PROCESSING

Computerized pattern evaluation; statistical analysis; results

Fig. 1 Flowchart for the pilot and the main study.

and evaporation, photographing of patterns, and data extraction and processing.

Preparation of Potencies

The preparation of 1x potencies followed the substance-specific guidelines[9,10] (►**Table 1**). Mineral powders and plant mother tinctures with manufacturing indication 1.1.8. (Ph. Eur.) were diluted in the ratio 1:9; 0.8 g of the substance was weighed and placed in a sterile glass cylinder (SBR-ET, Mix Cyl. 10 mL, B; Brand GmbH + CO KG, Wertheim, Germany) with stopper (untargeted volume 13 mL); subsequently 7.2 mL purified water according to Pharm. Eur. 9.4[9] ("purified water in bulk," X-SEPTRON LINE 10 VAL, BWT AQUA AG, Aesch, Switzerland) was added. By contrast, plant mother tinctures with manufacturing indications 1.1.3 and 1.1.5 (Ph. Eur.) were diluted in the first dilution step in the ratios 3:7 (to 2.4 mg substance, 5.6 mL water was added) and 2:8 (to 1.6 mg substance, 6.4 mL water was added), respectively. The cylinder was closed tightly and shaken by hand by performing 10 quick, vertical, movements in the air. Subsequent potencies (2x–6x) of all substances were prepared in the dilution ratio 1:9. After the settling of any foam, the cylinder was re-opened and 0.8 mL of the potentized solution was taken for the preparation of the next potency, as described previously. Water had to be used as solvent, since ethanol decreases the droplet's contact angle, which disturbs

the pattern formation. The potencies were prepared fresh for each experiment. The samples were prepared unblinded.

Preparation of Slides

Microscope slides of 76×26 mm (Menzel, pre-cleaned, cut edges, Thermo Scientific; Gerhard Menzel, B.V. & Co. KG, Braunschweig, Germany) were de-greased by washing them with a dishwasher liquid, then thoroughly rinsed with hot tap water, and placed in four consecutive purified water baths. Each slide was wiped dry with a laboratory wiper (Kimtech Science; Kimberly-Clark Professional, Roswell, Canada) just before droplet deposition.

Droplet Deposition and Evaporation

As depicted in ►**Fig. 2**, 3 µL droplets of the tested potency were deposited on a slide in two parallel rows, seven droplets per row, by the use of a micropipette of 20 µL capacity (Eppendorf Research Plus, Eppendorf, Hamburg, Germany). Evaporation took place in an incubator (KBF 720, cooled incubator with controlled humidity system, WTB Binder Labortechnik GmbH, Tuttlingen, Germany) with an inner plexiglass-chamber with a semi-permeable cover placed on a vibration absorbing base. In the inner chamber, 12 microscope slides were placed in three columns and four rows, and left for evaporation at 26°C and 44% relative humidity (rH) for 1 hour. In the main study, the slide distribution inside the chamber followed a quasi-

Table 1 Substances used in the pilot and main study, their origin, solute, and production method according to the European Pharmacopeia

Substance	Origin	Solute	Manufacturing
Pilot study			
Aurum chloratum (1x)	Mineral	H_2O	3.1.1 (Ph. Eur.)
Kalium bichromicum (2x)	Mineral	H_2O	3.1.1 (Ph. Eur.)
Natrium sulfuricum (powder)	Mineral	–	
Silicea (powder)	Mineral	–	
Zincum valerianicum (2x)	Mineral	Ethanol 100%	3.1.1 (Ph. Eur.)
Lilium tigrinum (Ø)	Plant	Ethanol 50% (v/v)	1.1.3 (Ph. Eur.)
Baptisia (Ø)	Plant	Ethanol 70% (v/v)	1.1.5 (Ph. Eur.)
Cimicifuga (Ø)	Plant	Ethanol 70% (v/v)	1.1.5 (Ph. Eur.)
Cypripedium pubescens (Ø)	Plant	Ethanol 70% (v/v)	1.1.5 (Ph. Eur.)
Echinacea (Ø)	Plant	Ethanol 70% (v/v)	1.1.5 (Ph. Eur.)
Ignatia (1x)	Plant	Ethanol 70% (v/v)	1.1.8 (Ph. Eur.)
Luffa (1x)	Plant	Ethanol 70% (v/v)	1.1.8 (Ph. Eur.)
Passiflora incarnata (Ø)	Plant	Ethanol 70% (v/v)	1.1.5 (Ph. Eur.)
Cocculus (1x)	Plant	Ethanol 90% (v/v)	1.1.8 (Ph. Eur.)
Valeriana (1x)	Plant	Ethanol 70% (v/v)	1.1.8 (Ph. Eur.)
Apis (1x)	Animal	Ethanol 70% (v/v)	Monograph (GHP)
Lachesis (2x)	Animal	Glycerol 85%	Monograph (GHP)
Spongia (1x)	Animal	Ethanol 70% (v/v)	1.1.9 (Ph. Eur.)
Main study			
Baptisia (1x)	Plant	Ethanol 70% (v/v)	1.1.5 (Ph. Eur.)
Echinacea (1x)	Plant	Ethanol 70% (v/v)	1.1.5 (Ph. Eur.)
Luffa (1x)	Plant	Ethanol 70% (v/v)	1.1.8 (Ph. Eur.)
Spongia (1x)	Animal	Ethanol 70% (v/v)	1.1.9 (Ph. Eur.)

Abbreviations: Ø—mother tincture; 1x, 2x—decimal dilutions; Ph. Eur.—European Pharmacopoeia; GHP—German Homeopathic Pharmacopoeia; 3.1.1, 1.1.3, 1.1.5, 1.1.8, 1.1.9—methods of preparation according to Ph. Eur.

randomization design to provide a uniform arrangement of the samples within the rows and to eliminate any gradients in the evaporating conditions within the chamber.

Photographing of Patterns

The droplet residues were photographed in dark field at magnification 100X using an optical microscope (Zeiss Laboratory.A1; Carl Zeiss Microscopy GmbH, Jena, Germany) with an attached camera (Moticam 5.0 MP; CMOS; Motic Electric Group Co., Ltd, Xiamen, China). In the pilot study, additionally bright-field and 25X, 50X, 200X, and 400X magnifications were used to photograph some structure details. The photographs were saved in jpeg format.

Droplets with disturbed crystallization due to presence of contaminating particles or due to edge effects on the slide were not photographed. In the main study, per experiment (one chamber-run, ►**Fig. 2**), 168 droplets were prepared (14 droplets × 12 slides). The three independent main experiments for the potencies 2x to 6x yielded 408, 448, 360, 359, and 359 images, respectively; the control experiments for potencies 2x to 4x yielded 128, 144, and 125 images, respectively. In total 2,331 images were subjected to the computerized pattern evaluation.

Data Extraction and Processing

Images deriving from the main study were analyzed by means of the software ImageJ (v. 1.50b) (National Institutes of Health, Bethesda, Maryland, USA)[11] with the plug-in Texture Analyzer (v. 04).[12] The analysis consisted of: (1) calculation of the GLD, which was performed on images subjected to a background extraction by means of the sliding paraboloid with rolling ball radius set at 50 pixels; and (2) calculation of the texture analysis parameters IDM and entropy on images subjected to a background extraction and converted into 8-bit type. Texture analysis was performed by running the GLCM algorithm, which is based on spatial dependence of pixels in a gray-level co-occurrence matrix with estimation of image features using second-order statistics, considering distances between pixel pairs of 4 pixels and angles of 90 degrees.

Statistical Analysis

The data deriving from the computerized image analysis were analyzed by means of analysis of variance (ANOVA) (one-way ANOVA with the factor randomization group, or two-way ANOVA with independent factors substance and experimental day, or row and column). In the case of two-way ANOVA, an interaction term between the independent factors was included in the statistical model to assess stability and reproducibility. All statistical calculations were performed with CoStat (v. 6.311) (CoHort Software, Monterey, California, USA).

Pairwise mean comparison was performed with the protected Fisher's least significant difference test (pairwise comparisons were evaluated only if the global F-test was significant at $p < 0.05$). This procedure gives a good safeguard against type I as well as type II errors, and thus balances well between false-positive and false-negative conclusions.[13]

Results

Pilot Study

The screening experiments showed that all 18 substances delivered patterns in all, or some, of the analyzed consecutive potencies up to 6x.

The patterns deriving from potencies of mineral origin (►**Fig. 3**) showed the greatest variety of forms, for instance: (1) creeping crystals, with ramifications extending outside the droplet with connection to the droplet border in
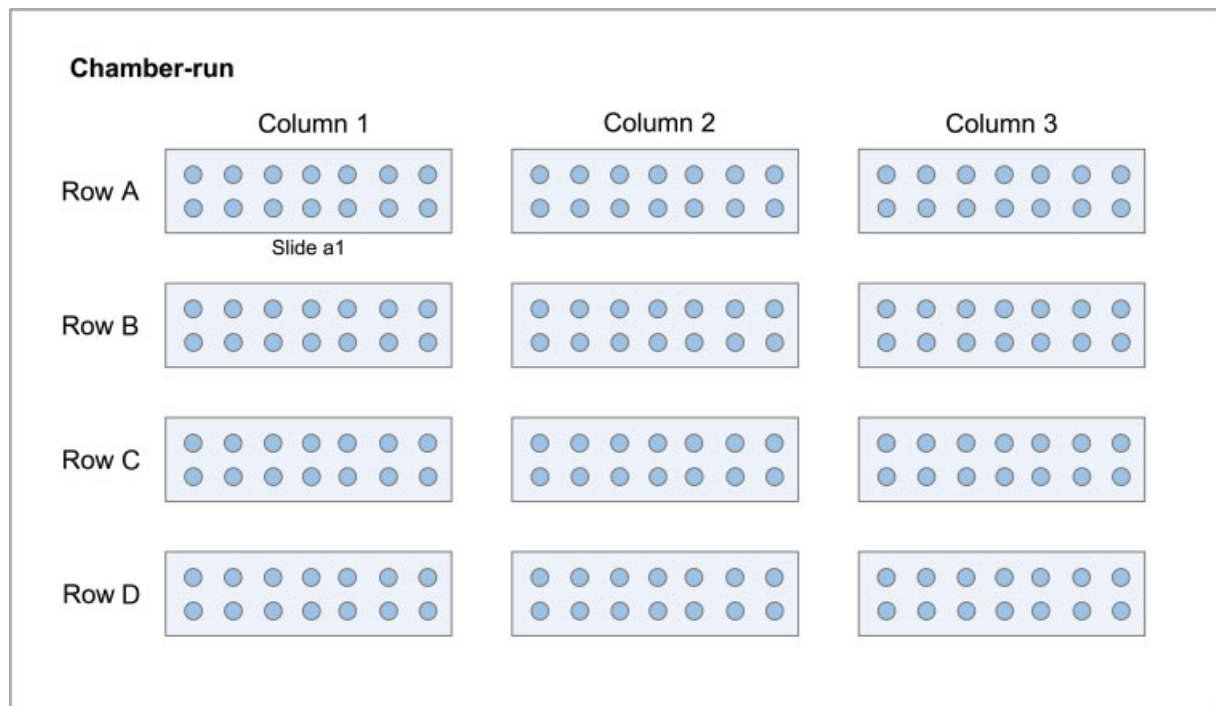
Fig. 2 Graphical representation of the chamber-run design. The evaporation chamber was organized in four rows (**A–D**) and three columns (1-3) in which 12 slides were placed (slide a1, a2, … d3). On each slide, 14 droplets were deposited for evaporation.

Natrium sulfuricum 2x (►**Fig. 3A**); (2) structures formed outside the droplet border without any visible connection to it, probably on diffusion basis in *Aurum chloratum* 2x (►**Fig. 3B**); (3) filament-like crystallization in *Aurum chloratum* 4x (►**Fig. 3C**); (4) crack patterns in *Silicea* 1x (►**Fig. 3D**); and (5) solid rhomboidal or cuboid-shaped crystals in *Zincum valerianicum* 3x and *Kalium bichromicum* 3x, respectively (►**Fig. 3E, F**). The patterns from potencies at different dilution levels prepared out of the same mineral substance also showed prominent differences between each other (e.g., *Kalium bichromicum* 3–5x in ►**Fig. 3G–I**, respectively).

The patterns from potencies of vegetal origin (►**Fig. 4A–I, K**) seemed to be more uniform. The 1x potencies showed transparent films (e.g., *Passiflora incarnata* 1x, ►**Fig. 4A**) or agglomerates as in *Cimicifuga* 1x (►**Fig. 4I**); also, thick film-like deposits with regular hexagonal spaces were noticed (*Cypripedium pubescens* 1x; ►**Fig. 4G**). Potencies in the range 2x to 4x showed in most cases (in 6 out of 10 vegetal substances) dendritic, ramified, fractal-like structures in the droplet center, as in *Passiflora* 2x to 4x and *Lilium tigrinum* 3x, 4x (►**Fig. 4B–F**); or (in 1 out of 10 vegetal substances), also placed in the droplet center, regular aggregates with branching, as *Cypripedium pubescens* 3x (►**Fig. 4H**).

Patterns from the analyzed potencies of animal origin (*Apis*, *Lachesis*, and *Spongia*) greatly resembled each other and contained mainly circles, probably formed as a result of step-wise shrinking of the droplet perimeter during evaporation (►**Fig. 4J**). *Lachesis* 3x could not be analyzed due to high glycerol content in the droplets, which prevented the evaporation.

The patterns showed substance-typical features in potency-range 1x to 3x and, albeit in smaller degree, also in 4x; patterns from mineral potencies showed in many cases

some substance-typical features also in 5x. Beyond this range, the patterns resembled those of pure solvent (e.g., *Echinacea* 5x in ►**Fig. 4K** and purified water in ►**Fig. 4L**).

For the main experimentation, we chose four substances, out of which three were of vegetal origin, creating dendritic, fractal-like structures in the droplet center in potencies 2x to 4x (*Baptisia* [B], *Echinacea* [E], and *Luffa* [L]), and one was of animal origin (*Spongia* [S]).

Differentiation Experiments

Visual Pattern Evaluation
Pattern examples formed in evaporated droplets of 2x to 6x potencies of B, E, L, and S are shown in ►**Fig. 5**. It can be seen that patterns obtained from the four substances differed remarkably at the potency levels 2x and 3x, and also—though somewhat less pronounced—at 4x. For potency levels 5x and 6x, the differences between the B, E, L, and S patterns ceased to be distinguishable, and the patterns resembled those of the solvent (purified water; ►**Fig. 4L**).

Computerized Pattern Evaluation
As shown in ►**Table 2**, the differences found between B, E, L, and S patterns by analyzing their GLD, IDM, and entropy by two-way ANOVA with independent factors substance and day were highly significant for the potency levels 2x (*F* values for the factor substance were highest) and decreased gradually with increasing the potency level. A clear differentiation of samples was possible until the potency 4x. For the potency levels 5x and 6x, the *F* values for the factor day were higher than those for the factor substance, which means that the day-to-day variation was larger than the influence of the substances
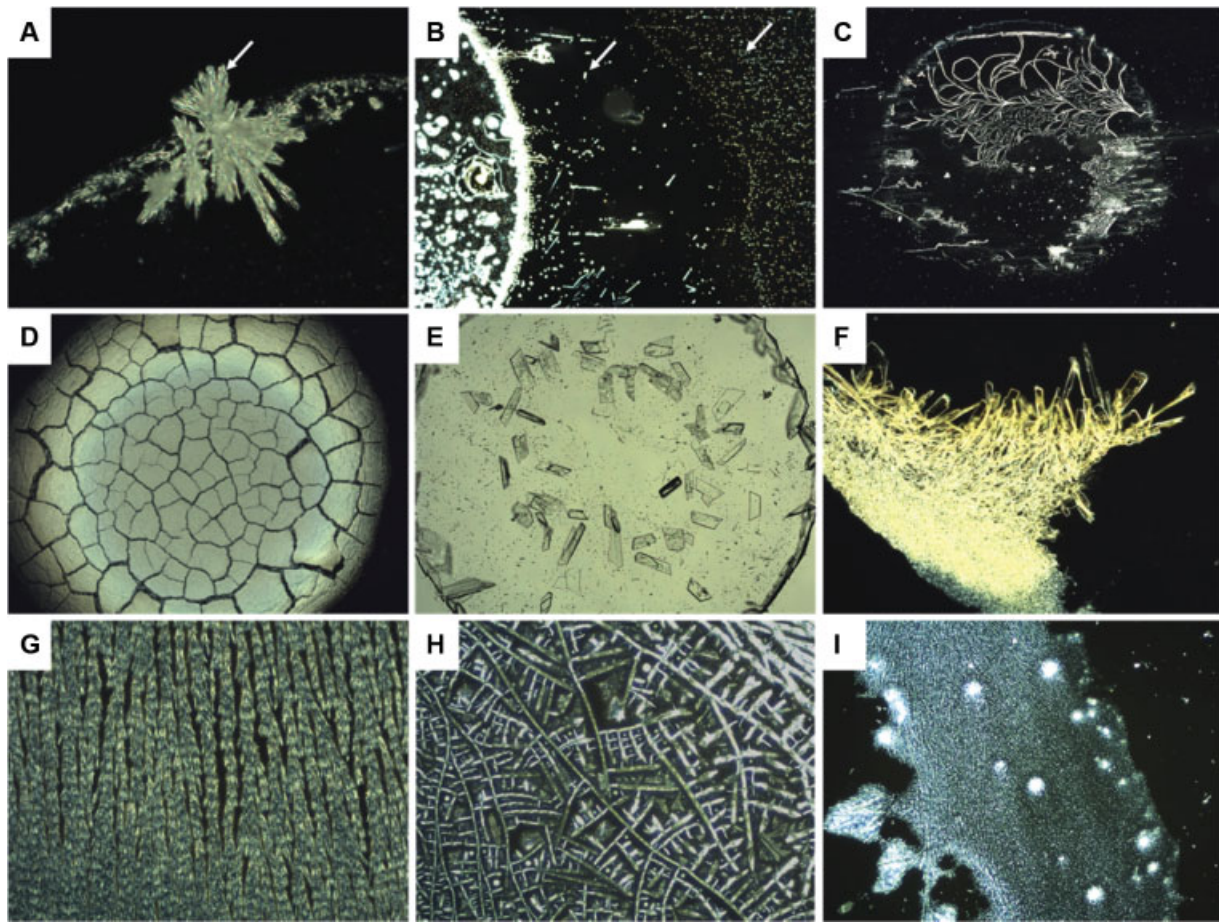
Fig. 3 Examples of pattern-forming phenomena in evaporating droplets of potencies of mineral origin: (**A**) creeping crystals (marked by an arrow) in *Natrium sulfuricum* 2x; (**B**) structures beyond the droplet border (marked by arrows), not connected to the droplet, in *Aurum chloratum* 2x; (**C**) filament-like structures in *Aurum chloratum* 4x; (**D**) cracks in *Silicea* 1x; (**E**) rhomboidal crystals in *Zincum valerianicum* 3x, (**F**) cuboid-shaped crystals in *Kalium bichromicum* 3x; and (**G–I**) examples of different textures in *Kalium bichromicum* 3x–5x, respectively. Images in magnification 25X (**D**); 50X (**B**, **C**); 100X (**E**); 200X (**A**, **F**); and 400X (**G–I**). Images are in dark field, with exception of (**E**) in bright field.

tested. For all potency levels, the interaction between the independent factors substance and day was highly significant, which means that the differences between B, E, L, and S varied to a certain extent for the individual experiments (►**Fig. 6**).

The mean values for the parameters GLD, IDM, and entropy for each investigated substance and dilution level are given in ►**Table 3**, alongside pairwise statistical comparison. For the potency level 2x, sample differentiation was possible for all three outcome parameters. For the potency level 3x, IDM was able to differentiate all samples, whereas entropy could not differentiate B and S, and GLD could not distinguish B, E, and S. For the potency level 4x, IDM and entropy did not distinguish between B and S; however, GLD ranked these two samples differently. For the potency levels 5x and 6x, some differences for two or three substances were significant; however, as shown by the *F*-values in ►**Table 2**—as also in ►**Fig. 6** depicting the results of GLD, IDM, and entropy for each substance within the three experimental days—these differences were not stable in the course of the experiments.

Positive Control Experiments
For the control experiments, we chose E2x, B3x, and L4x: that is, potencies that yielded fractal-like branch structures in the

potency range where the outcome parameters significantly differentiated most samples. The F-Test of ANOVA for the parameters GLD, IDM, and entropy of E2x, B3x, and L4x patterns from the control chamber runs (►**Table 4**) revealed that the position of the slides (independent factors row and column) inside the chamber (►**Fig. 2**) during evaporation had no significant influence on E2x; however, for B3x row and column were significant for two parameters, and for L4x the factor column was significant for all parameters. This means that row and/or column drifts may influence experimental outcome in the set-up chosen. Randomized allocation of the samples to row and column positions is therefore necessary to avoid systematic errors. Correspondingly, the applied randomization design eliminated the gradients for B3x and strongly decreased it for L4x (►**Table 4**).

►**Figure 7** compares the values of the pattern evaluation parameters GLD, IDM, and entropy for 2x to 4x potencies of B, E, L and S analyzed on the third experimental day (three slides per substance for each potency-level, placed randomly in the chamber) with the values for the control runs of E2x, B3x, and L4x (evaluated following the same randomization design). For example, in ►**Fig. 7**, graph 2x/GLD, the blue bars for L, E, B, and S indicate the mean values of GLD of L2x, E2x, B2x, and S2x
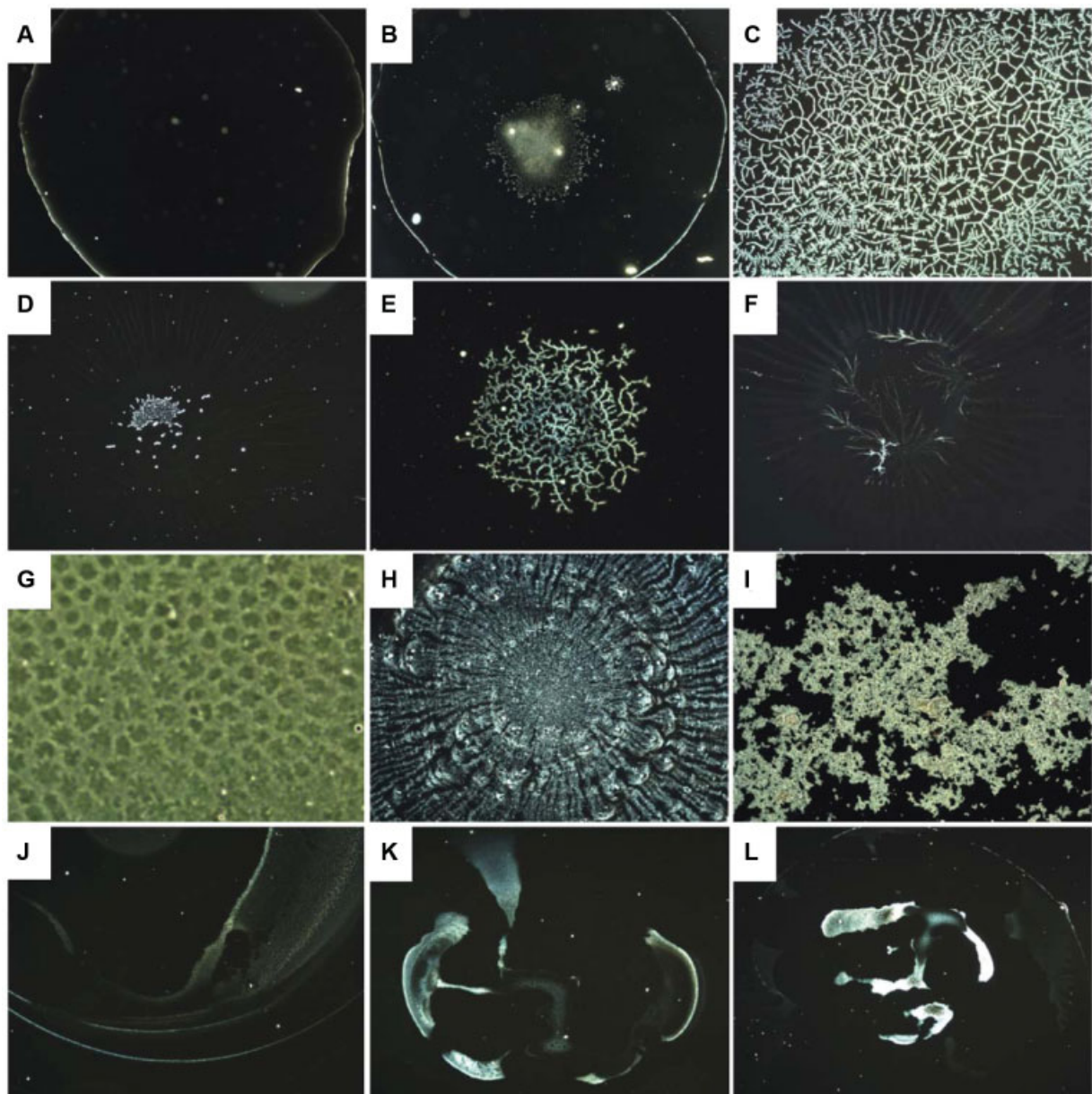
Fig. 4 Examples of structures formed in potencies of organic origin: (**A**, **B**) whole droplets without a structure and containing a fractal-like structure in *Passiflora incarnata* 1x and 2x, respectively; (**C**, **D**) fractal-like, branched structures in *Passiflora incarnata* 3x and 4x, and (**E**, **F**) *Lilium tigrinum* 3x and 4x; (**G**) hexagonal branched formations surrounded by a thick film in *Cypripedium pubescens* 1x; (**H**) organized, branched deposit in *Cypripedium pubescens* 3x; (**I**) agglomerates in *Cimicifuga* 1x; (**J**) circles due to stepwise evaporation in *Apis* 4x; and (**K**) structures in *Echinacea* 5x. (**L**) Example of structures formed in a droplet of purified water. Images in magnification 25X (**A–B**), 50X (**H**), 100X (**D–G**, **I–L**), and 200X (**C**). Images are in dark field, with exception of (**G**) in bright field.

evaporated on three slides each in one chamber run performed on the third experimental day, and the black symbols indicate the mean GLD values for the control E2x evaporated on slides placed in the same locations as L2x, E2x, B2x, and S2x in a control chamber run performed on the same day.

Discussion

Evaporation-Induced Pattern-Formation in Potencies of Mineral versus Organic Origin

The pilot study provided a wide range of structures formed during the droplet evaporation of the 18 investigated substances in consecutive decimal potencies up to 6x.

The structure formation in evaporating droplets may follow different scenarios depending on both the evaporation environment (e.g., temperature, relative humidity, pressure, substrate characteristics) and the droplet composition (e.g., substance and its degree of dilution, the liquid viscosity, electrical conductibility, droplet surface tension). In our experiments, the evaporation temperature and relative humidity were controlled and kept as constant as possible throughout all the experimental series; therefore, differences in patterns will rather depend on the droplet composition.

A visual inspection of the images revealed that potencies of mineral origin delivered the largest variety of structures (►**Fig. 3**), whereas in patterns obtained from vegetal and
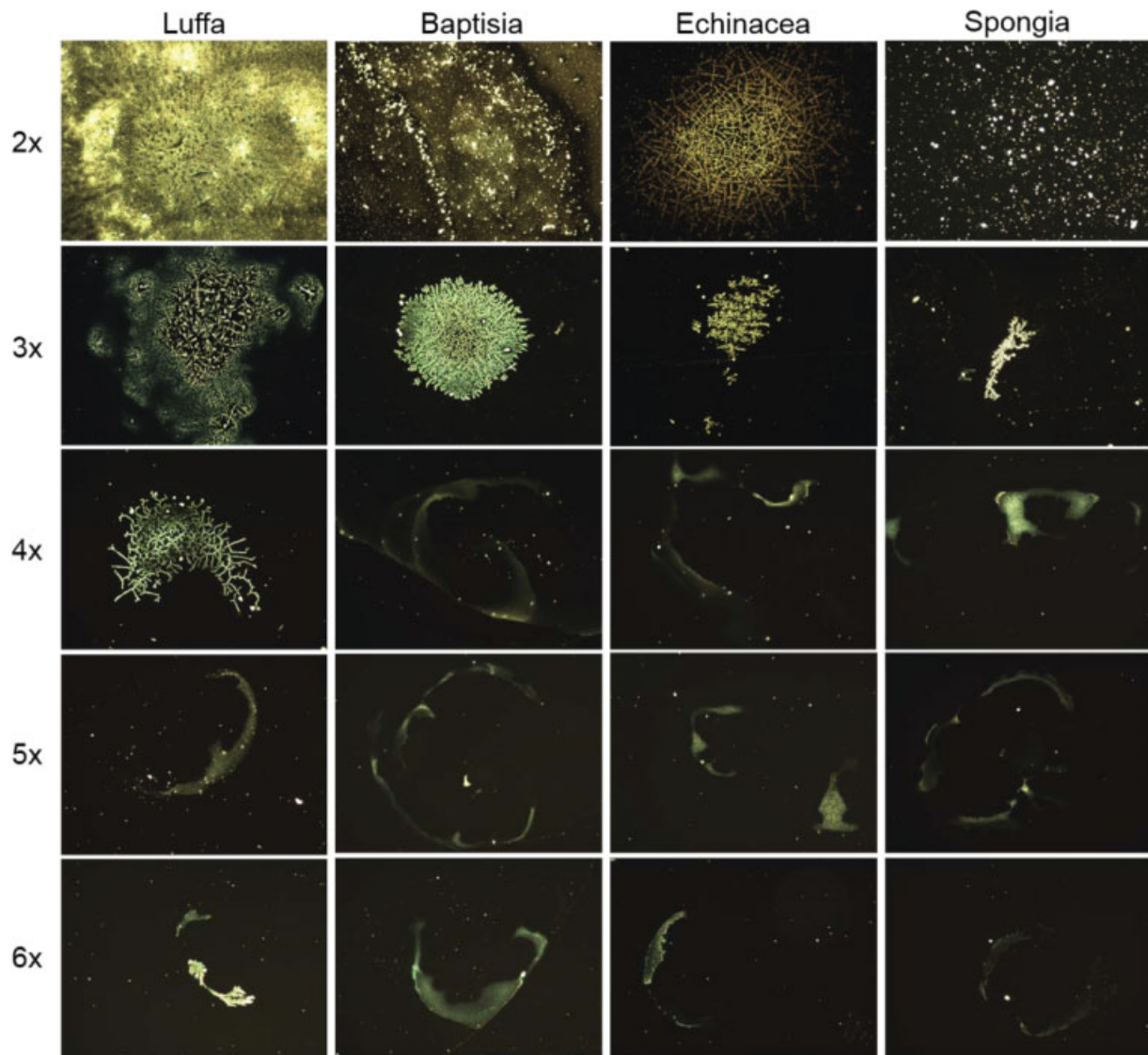
Fig. 5 Examples of the patterns formed during evaporation of droplets of potencies from *Luffa, Baptisia, Echinacea*, and *Spongia* in dilutions 2x–6x. Images in magnification 100X.

animal potencies this variety of observed forms was less marked (►**Fig. 4**). As regards potencies of mineral origin, out of the observation of forms it can be said that different pattern-forming mechanisms took place, involving *inter alia*: (1) classical crystal growth mechanisms relying on attachment of monomers and leading to the formation of solid, geometric crystals[14] (e.g., rhomboidal crystals in *Zincum valerianicum* 3x, ►**Fig. 3E**; cuboid-shaped crystals in *Kalium bichromicum* 3x; ►**Fig. 3F**); (2) formation of structures outside the droplet border (creeping crystals in *Natrium sulfuricum* 2x; ►**Fig. 3A**)[15] and formation of structures outside the droplet without any visible attachment to the droplet, probably on a diffusion basis (*Aurum chloratum* 2x; ►**Fig. 3B**); (3) formation of filament-like structures (*Aurum chloratum* 3x; ►**Fig. 3C**); and (4) formation of cracks due to tensions appearing in desiccating films (*Silicea* 1x; ►**Fig. 3D**).[16]

In potencies of vegetal origin, the predominant pattern-forming process seemed to be diffusion-limited aggregation relying on the attachment of clusters which, in the course of droplet evaporation, following Brownian motion, attach themselves to protruding structures leading to dendritic growth and the formation of so-called randomized fractals:[17,18] that is, branched structures. These structures were generally placed in the droplet center (►**Fig. 4B**) and their branches were thin and well-defined (►**Fig. 4C, E, F**), comparably thick (►**Fig. 4H**), or agglomerate-like (►**Fig. 4I**) (depending probably on the sizes and characteristics of the aggregating molecules).

As regards typical pattern-forming processes in potencies of animal origin, it is not possible to make a statement based on the present study, since it involved only three such potencies (*Apis, Lachesis*, and *Spongia*). However, all these potencies were characterized by very poor pattern-forming properties and created circles only, probably due to step-wise shrinking of the droplet perimeter during evaporation (►**Fig. 4J**).

Dendritic structures, similar to those obtained here from potencies of vegetal origin, have been observed also in

Table 2 The *F*-test results of the ANOVA for the parameters GLD, IDM, and entropy of droplet evaporation patterns obtained from *Baptisia, Echinacea, Luffa*, and *Spongia* in potency levels 2x–6x

	Substance		Experimentation day		Interaction substance x exp. day	
	F-Value	*p*-Value	*F*-Value	*p*-Value	*F*-Value	*p*-Value
Potencies 2x						
GLD	186.59	<0.0001***	0.72	0.4855	7.98	<0.0001***
IDM	930.75	<0.0001***	0.95	0.3856	9.09	<0.0001***
Entropy	684.52	<0.0001***	1.33	0.2666	11.13	<0.0001***
Potencies 3x						
GLD	170.99	<0.0001***	22.88	<0.0001***	5.09	<0.0001***
IDM	312.93	<0.0001***	12.73	<0.0001***	9.05	<0.0001***
Entropy	354.31	<0.0001***	16.69	<0.0001***	8.15	<0.0001***
Potencies 4x						
GLD	195.73	<0.0001***	1.61	0.2010	3.83	0.0010**
IDM	154.83	<0.0001***	2.51	0.0825	8.26	<0.0001***
Entropy	172.90	<0.0001***	1.93	0.1461	7.35	<0.0001***
Potencies 5x						
GLD	1.19	0.3115	2.37	0.0948	3.95	0.0008***
IDM	3.58	0.0142*	22.82	<0.0001***	8.97	<0.0001***
Entropy	3.13	0.0258*	18.30	<0.0001***	8.85	<0.0001***
Potencies 6x						
GLD	4.54	0.0039**	24.55	<0.0001***	9.00	<0.0001***
IDM	4.85	0.0025**	61.61	<0.0001***	14.02	<0.0001***
Entropy	6.81	0.0002***	60.72	<0.0001***	16.53	<0.0001***

Abbreviations: ANOVA, analysis of variance; GLD, gray-level distribution; IDM, inverse difference moment.
Note: Effects of *substance* and *experimentation day* as well as their interaction are given for each parameter and potency level
(*$p < 0.05$; **$p < 0.01$; ***$p < 0.001$).

previous studies regarding DEM applied to wheat seed leakages,[3–6,19,20] where this specific kind of crystallization showed to be sensitive toward stress induced by poisoning,[20] homeopathic treatment influences,[3,5] the number of strokes applied in-between the dilution steps,[6] and force-like effects of homeopathic preparations.[4] In these studies, the use of a biological model (wheat seed leakage model) enabled work with high potencies. The results obtained showed a correlation with wheat seed viability, indicating that the droplet pattern characteristics corresponded to the biological effects of the applied treatment. In the present study on low potencies, we applied DEM as a physical model to characterize the physico-chemical properties of the tested substances.

Based on past experience, we decided to concentrate on dendritic structures also in the present investigation of low potencies *per se*. Therefore we chose for the main study three substances of vegetal origin (*Baptisia, Echinacea*, and *Luffa*) due to their ability to create dendritic, fractal-like structures in the droplet center in the potency range 2x to 4x. To complement these three substances of vegetal origin with one substance of animal origin, we further added *Spongia* to the main study.

Differentiation of Potencies in Range 2x to 6x

In the differentiation experiments of the four substances B, E, L and S in dilutions from 2x to 6x, DEM showed to be discriminative for the potency levels 2x to 4x, whereas in 5x and 6x differences due to the substance could no longer be detected (►**Fig. 4K**), and the patterns resembled those of pure solute (purified water; ►**Fig. 4L**). As shown in ►**Table 2**, the *F* values from ANOVA for the factor substance were high for the potencies 2x to 4x (from 170 to 930) and larger than those for the factor day and the interaction between the two factors substance and day; for the potencies 5x and 6x, this ratio reversed and the *F* values for the factor substance were smaller than those of the factor day and the interaction between substance and day.

For the potency level 4x, the differentiation between B and S was possible only by one pattern evaluation parameter (GLD), and it was visually apparent that the patterns of these two potencies resembled the pattern of pure solute (►**Fig. 4L**, ►**Fig. 5**). It therefore may be supposed that the limit of DEM's ability to differentiate between potencies of different origin may depend on the substance characteristics.
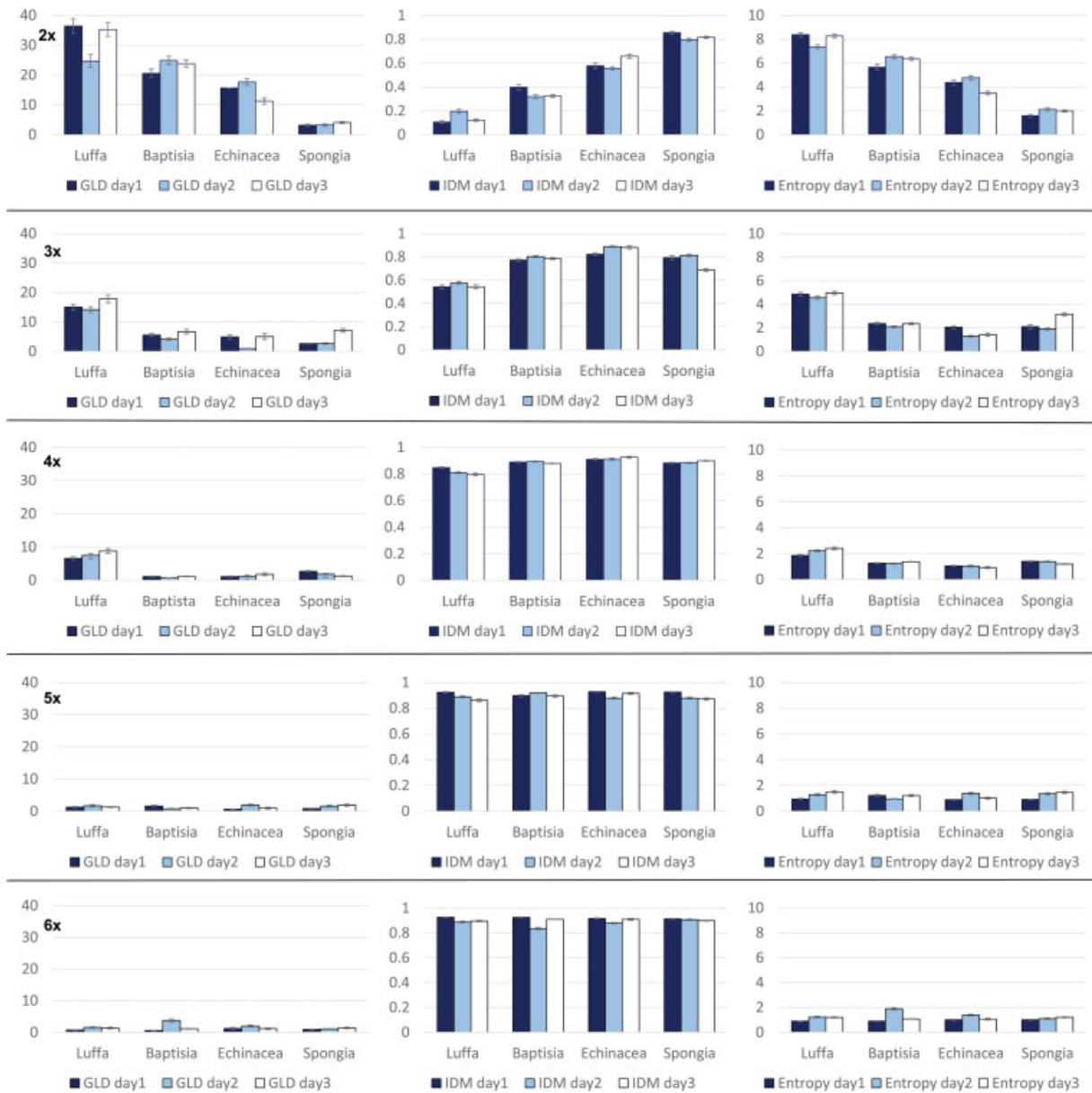
Fig. 6 Graphical representation of the results (mean values ± standard error) of the parameters *gray-level distribution* (GLD; left graphs), *inverse difference moment* (IDM; middle graphs), and *entropy* (right graphs) for 2x–6x potencies of *Luffa, Baptisia, Echinacea*, and *Spongia* (rows) on the three experimentation days.

Repeatability of the Experiments and Robustness of the Model

The differentiation experiments were performed on 15 different days (3 days for each potency level 2x to 6x). As can be seen in ►**Fig. 6**, the reproducibility was quite good for the potency levels 2x to 4x, whereas for 5x and 6x the samples could no longer be differentiated. It is worthy of notice that there were significant inversions of the substance effect between the experimentation days for all potency levels (►**Table 2**). Such inversions may be due to: (1) some methodological or technical instability, in which case they might be eliminated by further optimization of the experimental design and work flow; or (2) some—in this experiment uncontrolled—external factors modifying the pattern of the potency response in the DEM model.

In the potency range 2x to 4x for the four substances, the robustness of DEM was scrutinized by means of control experiments, which were designated as chamber runs with only one potency, E2x, B3x, and L4x. These control experiments revealed that there were gradients in the chamber, probably due to slight differences in evaporation conditions (temperature, relative humidity), causing differences in the patterns deriving from different positions within the chamber. To neutralize these effects, the slide distribution followed a quasi-randomization design to provide a possibly uniform distribution of the sample replicates within the chamber rows and columns (►**Fig. 2**), avoiding at the same time two sample replicates being deposited on slides lying nearby. As shown in ►**Table 4**, for the potencies 3x and 4x the factor row had a strong significant influence on the pattern

Table 3 Mean values of the parameters GLD, IDM, and entropy for 2x–6x potencies of *Luffa*, *Baptisia*, *Echinacea*, and *Spongia*

	N	GLD	IDM	Entropy
Potencies 2x				
Luffa	103	32.217 (a)	0.141 (d)	8.008 (a)
Baptisia	101	22.961 (b)	0.348 (c)	6.162 (b)
Echinacea	109	15.061 (c)	0.594 (b)	4.253 (c)
Spongia	95	3.573 (d)	0.826 (a)	1.871 (d)
Potencies 3x				
Luffa	115	15.715 (a)	0.552 (d)	4.796 (a)
Baptisia	100	5.451 (b)	0.787 (b)	2.265 (b)
Echinacea	111	3.788 (c)	0.863 (a)	1.585 (c)
Spongia	122	4.263 (bc)	0.758 (c)	2.453 (b)
Potencies 4x				
Luffa	90	7.623 (a)	0.817 (c)	2.163 (a)
Baptisia	90	0.993 (c)	0.887 (b)	1.292 (b)
Echinacea	90	1.364 (bc)	0.915 (a)	1.015 (c)
Spongia	90	1.939 (b)	0.888 (b)	1.330 (b)
Potencies 5x				
Luffa	92	1.398 (a)	0.890 (c)	1.244 (a)
Baptisia	89	1.089 (a)	0.903 (ab)	1.125 (ab)
Echinacea	90	1.155 (a)	0.906 (a)	1.097 (b)
Spongia	88	1.415 (a)	0.892 (bc)	1.240 (a)
Potencies 6x				
Luffa	91	1.192 (b)	0.903 (a)	1.105 (b)
Baptisia	90	1.789 (a)	0.890 (b)	1.287 (a)
Echinacea	89	1.436 (ab)	0.902 (a)	1.149 (b)
Spongia	89	1.089 (b)	0.906 (a)	1.103 (b)

Abbreviations: N, number of droplet patterns; GLD, gray-level distribution; IDM, inverse difference moment.
Note: a, b, c, d (per quartet of means of the different substances at a given potency), differing letters: statistical differences between involved groups at $p < 0.05$; same letters: absence of statistical differences between involved groups ($p > 0.05$).

evaluation parameters (also the factor column for the textural parameters for 3x); this influence could be neutralized in the randomization group. ►**Figure 7** depicts additionally the differences between the B, E, L, and S samples for the same potency dilution as the control samples evaluated with the same randomization design. Future experiments should include further optimization of the chamber set-up to minimize or eliminate these gradients.

Future Perspectives

Low homeopathic potencies represent an interesting field of study, providing the possibility to investigate the material that is still present in these dilution levels, thus shedding new light on the procedure of homeopathic potentization by investigating the effects of the first dilution/succussion steps on the material potentized.

In the present study, we showed that DEM applied to potencies *per se* was able to differentiate phenomenologically between potencies derived from different substances in the potency range 2x to 4x. In this investigation, only one batch of each substance was studied. Further investigations will have to compare independent batches (mother tinctures prepared from material from different harvesting years and/or areas) to determine possible generalization from the differences between mother tinctures as observed in this study.

Further investigations could include questions such as: (1) effects related to the physical processes applied during potency preparation (potentization manner [manual versus mechanical]; potentization intensity [number of applied strokes]; possible influence of the potentization vessel [shape and material]); (2) effects related to the time (hour/day/month) of potency preparation; (3) influence of the storage on the potency; and (4) contribution of single remedies to the patterns formed by homeopathic combination medicines.

The different, non-dendritic, pattern-forming phenomena observed in the pilot study in potencies of mineral origin —for instance the classical nucleation mechanism, creeping

Table 4 Analysis of variance of the control experiments

	Column		Row		Interaction column x row		Randomization group	
	F-Value	p-Value	F-Value	p-Value	F-Value	p-Value	F-Value	p-Value
Echinacea 2x								
GLD	0.49	0.6147	2.16	0.0967	2.51	0.0252*	2.94	0.0356*
IDM	1.75	0.1790	2.59	0.0563	1.00	0.4253	0.75	0.5236
Entropy	1.53	0.2211	2.46	0.0658	1.35	0.2422	0.87	0.4565
Baptisia 3x								
GLD	1.48	0.2312	4.76	0.0035**	3.68	0.0020**	0.32	0.8078
IDM	13.32	<0.0001***	6.95	0.0002***	4.70	0.0002***	1.55	0.2046
Entropy	7.50	0.0008***	1.71	0.1664	4.84	0.0002***	2.08	0.1059
Luffa 4x								
GLD	0.62	0.5383	6.46	0.0004***	1.63	0.1433	3.43	0.0192*
IDM	1.22	0.2991	12.38	<0.0001***	2.87	0.0123*	2.49	0.0633
Entropy	0.82	0.4432	11.04	<0.0001***	2.50	0.0262*	2.16	0.0963

Abbreviations: GLD, gray-level distribution; IDM, inverse difference moment.
Note: F-test results for the parameters GLD, IDM, and entropy of patterns obtained in three control chamber-runs (*Echinacea* 2x, *Baptisia* 3x, and *Luffa* 4x) for the factors column, row, their interaction, and for the randomized group allocation (* $p < 0.05$; ** $p < 0.01$; *** $p < 0.001$).
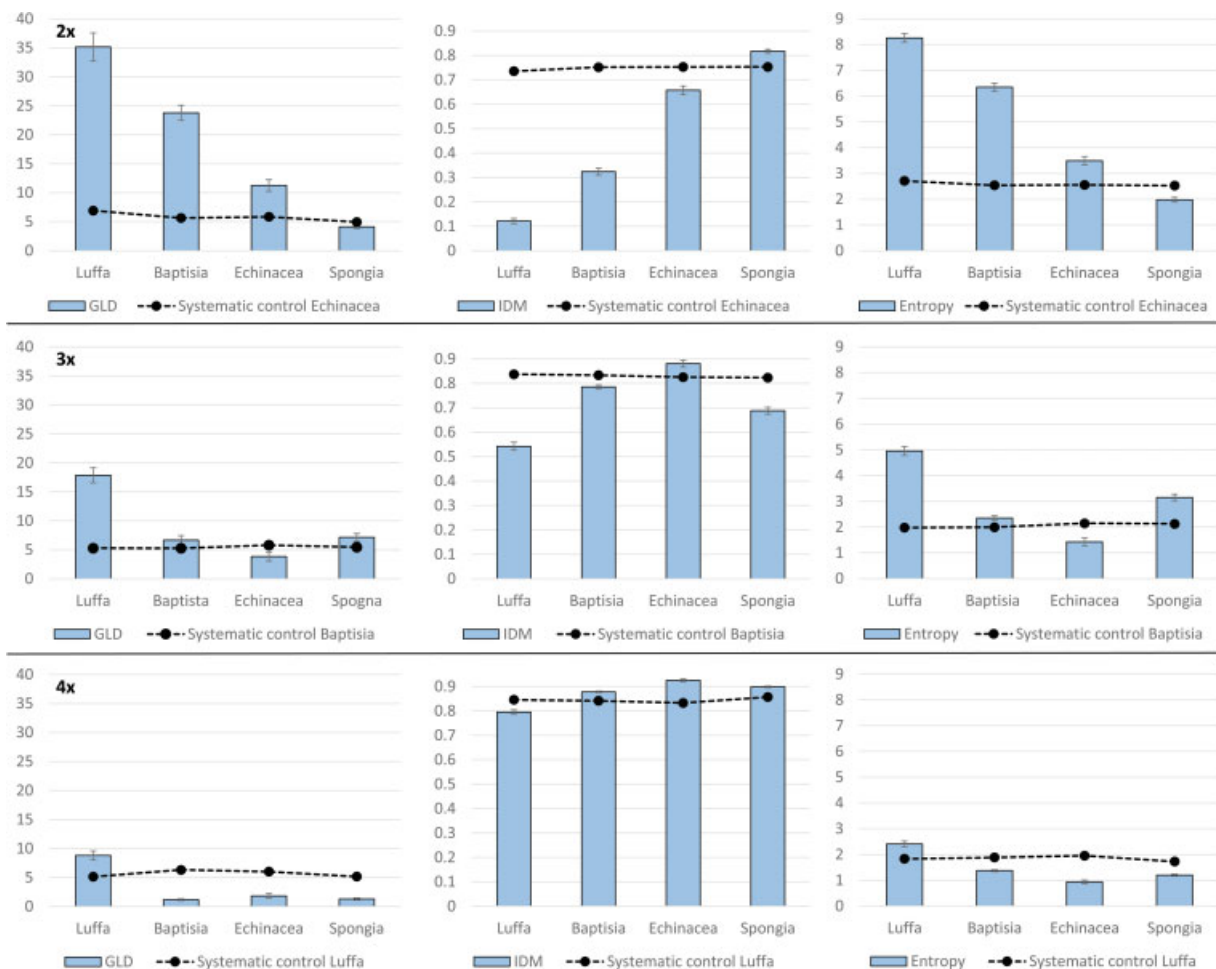
Fig. 7 Graphical representation of the mean values (± standard error) of the parameters *gray-level distribution* (GLD; left graphs), *inverse difference moment* (IDM; middle graphs), and *entropy* (right graphs) for the potencies 2x–4x for *Luffa, Baptisia, Echinacea*, and *Spongia* (blue bars) and for the controls *Echinacea* 2x (upper row), *Baptisia* 3x (middle row), and *Luffa* 4x (lower row), (black markers, and lines), evaporated in the same chamber positions as the respective potencies.

crystals, and cracks (►**Fig. 3**)—represent also an interesting and new field of investigation. So far, all methods based on evaporation-induced pattern formation applied in homeopathic basic research have concentrated on fractal structures formed in the course of diffusion-limited aggregation (e.g., dendritic structures); it is not known if other non-dendritic pattern-forming phenomena might also be sensitive to the effects of potencies.

Conclusions

In the present study, we proposed DEM for the first time for analyzing low potencies *per se* and showed that the evaporation-induced pattern formation in droplets may represent a suitable tool for their phenomenological characterization, due to the fact that they still contain material. Formation of patterns in evaporating droplets has previously been used to analyze effects of high and ultra-high potencies by means of experimental models including test organisms, or applying a sequence of droplets dried one on another residue. Low potencies, retaining enough material for the pattern formation, allow the application of the method without the use of any test organisms or additives. The reported experimental protocol may serve as a basis for further studies in this field, such as comparison of potencies versus dilutions, or studies on homeopathic combination remedies with regard to the influence their single remedy components may have on the pattern of different mixtures.

Highlights
- Droplet evaporation patterns from potencies of mineral origin show a great variety of forms.
- Patterns from potencies of vegetal origin show rather dendritic structures typical for diffusion-limited aggregation.
- Computerized pattern evaluation allowed us to differentiate between potencies deriving from different substances until 4x.
- Patterns from 5x and 6x potencies resembled the pattern of control water.
- The droplet evaporation method might serve to analyze the matter still present in low potencies and how it changes during consecutive potentization steps.

Conflict of Interest
None declared.

References

1 Hahnemann S. Organon of Medicine. 6th ed. London: Headland; 1849
2 Kokornaczyk MO, Scherr C, Bodrova NB, Baumgartner S. Phase-transition induced pattern formation applied to basic research in homeopathy: a systematic review. Homeopathy 2018;107:181–188
3 Kokornaczyk MO, Trebbi G, Dinelli G, et al. Droplet evaporation method as a new potential approach for highlighting the effectiveness of ultra high dilutions. Complement Ther Med 2014; 22:333–340
4 Kokornaczyk MO, Baumgartner S, Betti L. Preliminary study on force-like effects between As45x, water, and wheat seeds performed by means of the droplet evaporation method. Int J High Dilution Res 2015;14:17–19
5 Kokornaczyk MO, Baumgartner S, Betti L. Polycrystalline structures formed in evaporating droplets as a parameter to test the action of *Zincum metallicum* 30c in a wheat seed model. Homeopathy 2016;105:173–179
6 Betti L, Trebbi G, Kokornaczyk MO, et al. Number of succussion strokes affects effectiveness of ultra-high-diluted arsenic on in vitro wheat germination and polycrystalline structures obtained by droplet evaporation method. Homeopathy 2017;106:47–54
7 Elia V, Ausanio G, Gentile F, Germano R, Napoli E, Niccoli M. Experimental evidence of stable water nanostructures in extremely dilute solutions, at standard pressure and temperature. Homeopathy 2014;103:44–50
8 Lo SY, Geng X, Gann D. Evidence for the existence of stable-water-clusters at room temperature and normal pressure. Phys Lett A 2009;373:3872–3876
9 European Pharmacopoeia, Ninth Ed, Supplement 9.4. EDQM, editor. Strasbourg, France: Council of Europe; 2017
10 Medpharm Scientific Publishers. German Homoeopathic Pharmacopoeia (GHP) – including 14th Supplement. Stuttgart, Germany: Medpharm Scientific Publishers; 2017
11 Collins TJ. ImageJ for microscopy. Biotechniques 2007;43:25–30
12 Cabrera JE. Texture Analyzer. 2006. Available at: https://imagej.nih.gov/ij/plugins/texture.html. Accessed April 11, 2018
13 Carmer SG, Swanson MR. An evaluation of ten pairwise multiple comparison procedures by Monte Carlo Methods. J Am Stat Assoc 1973;68:66–74
14 Waychunas GA. Structure, aggregation and characterization of nanoparticles. Rev Mineral Geochem 2001;44:105–166
15 van Enckevort WJP, Los JH. On the creeping of saturated salt solutions. Cryst Growth Des 2013;13:1838–1848
16 Lee WP, Routh AF. Why do drying films crack? Langmuir 2004; 20:9885–9888
17 Sosso GC, Chen J, Cox SJ, et al. Crystal nucleation in liquids: open questions and future challenges in molecular dynamics simulations. Chem Rev 2016;116:7078–7116
18 Wu J, Li Z. Density-functional theory for complex fluids. Annu Rev Phys Chem 2007;58:85–112
19 Kokornaczyk MO, Dinelli G, Marotti I, Benedettelli S, Nani D, Betti L. Self-organized crystallization patterns from evaporating droplets of common wheat grain leakages as a potential tool for quality analysis. Scientific World Journal 2011;11:1712–1725
20 Kokornaczyk MO, Dinelli G, Betti L. Approximate bilateral symmetry in evaporation-induced polycrystalline structures from droplets of wheat grain leakages and fluctuating asymmetry as quality indicator. Naturwissenschaften 2013;100:111–115